

Steadily-rotating overdriven detonation : comparison of experiments with Geometrical Shock Dynamics modeling

C. Jourdain, V. Rodriguez, P. Vidal, R. Zitoun
Institut Pprime, UPR 3346 CNRS, Fluid, Thermal and Combustion Sciences Department
ENSMA, BP 40109, 86960 Futuroscope-Chasseneuil, France

1 Introduction

Propulsion by detonation has been studied for several decades because of its higher theoretical thermal efficiency compared to the isobaric combustion mode. Most studies consider the rotating-detonation mode, but uncertainties on the actual wave dynamics still makes the optimum choice of the chamber inner geometry a subject of investigations. Rotating detonation chambers can be annular or hollow, i.e., with or without a cylindrical center body, or semi-hollow, i.e., with a conical center body. Although only a limited number of experiments is available, the hollow and semi-hollow configurations appear to produce larger pressures and velocities, and an interpretation is that burned gases expand more easily and heat losses at walls are smaller [1,2]. The present work is an investigation into the semi-hollow configuration by means of a single-shot model experiment by which a detonation is transmitted from a straight channel to a curved chamber with a small center body. The detonation dynamics inside the chamber is characterized by means of soot-foil recordings and high-speed schlieren, shadowgraphy and direct-light visualizations. The main finding is a steadily-rotating overdriven Mach detonation regime along the chamber outer wall, depending on initial pressure. A continuously-rotating overdriven detonation could be a promising regime because of the larger pressures it generates. In the numerical part of this study a rather good agreement of experiments with modeling by means of Whitham's Geometrical Shock Dynamics (GSD) modeling is obtained, albeit only qualitatively at this time. This supports our former interpretation that this specific regime is essentially self-similar, and thus mostly driven by geometry, and not by chemical kinetics [3,4].

2 Set-up and experimental results

Figure 1 shows a schematics of the experimental set-up. The main two elements are the semi-hollow curved chamber and a straight cylindrical detonation tube in which detonation was generated before transmission to the chamber. The latter was fixed at one end of the tube, and a premixed reactive gas was ignited at the other end by means of an exploding wire. The tube length and inner diameter were 2 m and 51 mm, respectively. A 500-mm long Shchelkin spiral was positioned at the ignition end of the tube in order to enhance detonation build-up and obtain the Chapman-Jouguet (CJ) regime before detonation enters the chamber. The regime was checked from signals of four Kistler 603B piezoelectric sensors (P1-P4 in Fig. 1) set at the tube exit end opposite to ignition, and cross-checked from detonation cell size measurements on a sooted foil also set at this end. The chamber had a 20-mm height and an 80-mm radius outer wall, and its entry channel had a $20 \times 30\text{-mm}^2$ cross-section. The chamber exit channel opened into a dump tank which it was separated from

by a Mylar thin sheet replaced after each shot, before vacuuming the set-up and injecting the reactive gas up to the desired initial pressure. The chamber was designed so as to implement either soot-foil recordings or schlieren, shadowgraphy and low-pass filtered direct-light high-speed visualizations using a Shimadzu HPV-2 camera. For the soot recordings, the upper and lower faces of the chamber were steel plates with inner sides lined with polished steel foils. For the schlieren and shadowgraphy visualizations, the upper and lower faces of the chamber were made of $215 \times 275\text{-mm}^2$, 27-mm thick optical Borosilicate Crown glass (BK-7) with a visualization surface larger than the chamber diameter. The visualization surface was discretized in four zones, each investigated in separate experiments. The sampling rates and the exposure time were 0.5 or 1 Mfps and 250 ns, respectively. For the direct-light visualizations, the chamber upper and lower faces were an optical BK-7 window and a darken metal sheet, respectively, the filter had a 600-nm cut-off wave length, and the exposure time was set to 125 ns. All experiments were carried out with the stoichiometric propane-oxygen mixture ($C_3H_8 + 5 O_2$) with initial pressure p_0 ranging from 8 kPa to 15 kPa and initial temperature $T_0 = 288 \text{ K} \pm 5 \text{ K}$.

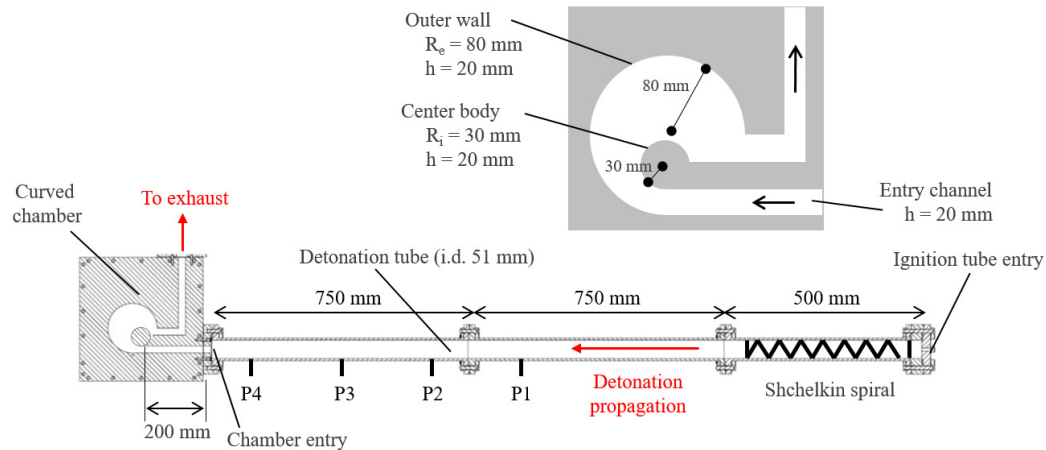


Figure 1: Set-up schematics showing the curved chamber and the detonation tube.

The experiments reveal the existence of an initial-pressure range for which an irregular transmission mode of detonation is achieved. This mode is the steady rotation of a detonation front normal to the chamber outer wall. Below the lower limit of this p_0 range, detonation quenches, above the upper limit, detonation re-initiates in the whole chamber without rotating (regular transmission). Figure 2-left is a typical shadowgraph sequence of an irregular transmission, with time increasing rightward from the top, and 2-right is a typical soot recording, both for $p_0 = 12 \text{ kPa}$. The upper first shadowgraph picture shows the CJ cellular detonation immediately after transmission from the ignition tube to the chamber entry channel. The upper second, third and fourth pictures cover the domain where the transient phenomena associated with successive detonation quenchings and re-initiations take place. These transients are triggered by the detonation diffraction at the end of the entry channel end, where the rounding of the centerbody begins. The upper second and third pictures show details of the diffraction process. An expansion wave propagates outward along the front surface and increases the reaction time as indicated by the thickening of the dark line representing the front and the spreading of the gradient domain behind it. Depending on p_0 , detonation may successively fully quench and re-initiates at these angular positions. The upper fourth picture shows a typical re-initiation attempt with, in particular, a triple point propagating downward from the outer wall. The lower pictures show the last successful re-initiation with the installation and the rotation of the detonation front.

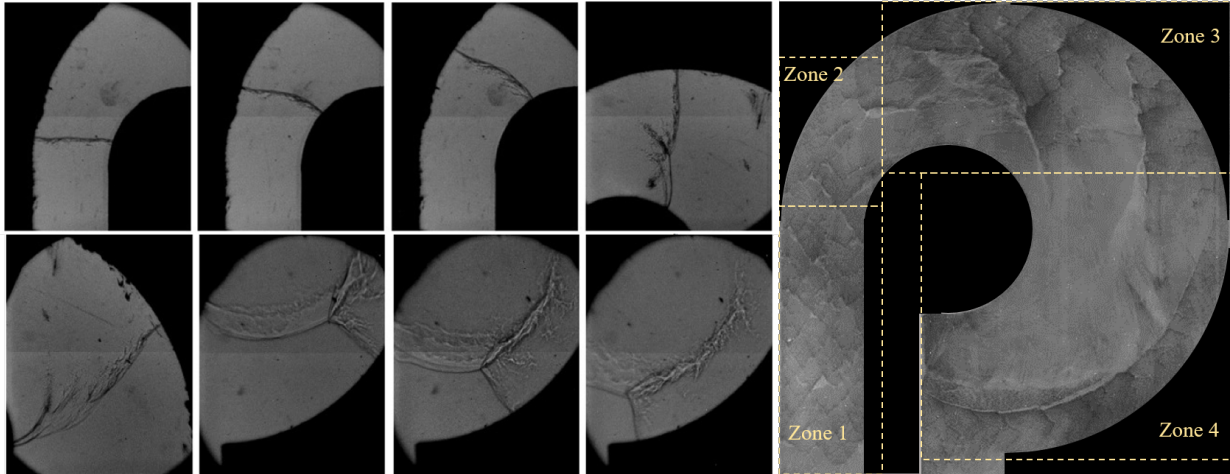


Figure 2: Irregular transmission mode ($p_0 = 12$ kPa). Left : shadowgraph sequence (time increases rightward from the top), right : soot recording.

The lower rightmost three pictures show the rotation of the detonation front normal to the outer wall. The configuration is a typical 3-fronts Mach wave. A physical interpretation of this specific detonation regime is obtained from an analogy with the generic situation where an incident shock initially propagating normal to a flat surface comes to interact with a compressive wedge [5]. Depending on the wedge angle, a Mach stem may form at the wedge tip, with a triple point moving away from the tip, along the incident shock. In the present work, the incident front is the curved shock originating from diffraction, the reflected front is the detonation normal to the wall, and the third shock is the thin dark line above the unstable contact surface in the form of the spread gradient domain behind the triple point. The speed at which the triple point moves away from the outer wall can thus be equal to the relative speed at which the wall would move away from the reference line tangent to the wall at the current front position, so the Mach detonation front has a constant height. In the relative frame moving with the rotating front, this phenomenon is also similar to that of a shock propagation in a continuously-converging channel, so the front is continuously overdriven. The quantitative analysis of the front positions as a function of angular position unambiguously indicates that the normal velocity to the Mach front at the wall is larger than the Chapman Jouguet velocity for the considered initial pressure. The soot recordings also show unambiguously that these Mach fronts have the typical cellular structure of gaseous detonations. The cell mean width is much smaller than those on the CJ detonation front in the chamber entry channel, which constitutes another indication that the Mach front in these experiments is an overdriven detonation. Measurements give cell mean widths for the CJ detonation and the overdriven detonation equal to 10 mm and 1 mm, respectively. Indeed, the larger the front velocity is, given the initial pressure, the larger the temperature at the detonation leading shock, and, thus the smaller the characteristic chemical time and the cell mean width are. Schlieren and shadowgraph techniques cannot return information on chemical composition, so it is difficult to assess the reactivity magnitude behind the diffracted shock. Nevertheless, the domain behind this curved shock can be considered to be weakly reactive, if not, inert. The soot recordings indeed show the same continuous aspect of the domain above the Mach band, starting from the diffraction point. Therefore, admitting that reaction is considerably slowed down at the diffraction point, if not essentially quenched, implies admitting a very weakly reactive flow behind the diffracted wave at further positions. Similarly, the visualizations do not show any perturbations ahead of the Mach front and the diffracted shock, which thus propagate in the initial fresh gas at p_0 .

3 Geometrical Shock Dynamics modeling

Because of the constant-angular velocity and the negligible size of the detonation cell mean width on the Mach front, this specific overdriven rotating detonation regime appears to be essentially self-similar, so the dominant effect determining the wave dynamics would be that of the wall geometry. This suggests implementing the simple model of Whitham's Geometrical Shock Dynamics (GSD) [6–8]. The model is a tracking technique that returns the shock shapes and positions upon changes of lateral boundaries. These shapes and positions are obtained by integrating a differential equation relating the variations of the shock Mach number M and the relative variation of the shock local area A (the local total curvature). The A - M relation is a differential equation resulting from an analysis of the Euler balance laws for inviscid compressible non-reactive flows that essentially amounts to considering that the combination $\partial p/\partial t + \rho c \partial u/\partial t$ of time partial derivatives remains negligibly small upon changes of lateral boundary conditions. The consequence is that the exact compatibility relation between total derivatives along the forward-facing acoustic paths is then very well approximated by the same combination of total derivatives along the shock path which constitutes the A - M relation. Since the original formulation, several elaborations have been considered, and this work implements that of Milton [9]. Its interest is to be capable of handling interaction terms, that is, perturbations along the positive characteristics by a reflected shock and a contact surface. The modeling then capture and track triple points more precisely as shown in [10] and as we checked it in our validation cases. The A - M relation in our modeling writes

$$\frac{dA}{A} + \left[\frac{2M}{\lambda(M)(M^2 - 1)} + \frac{\eta}{M} \right] dM = 0, \quad (1)$$

$$\lambda(M) = \left(1 + \frac{2}{\gamma + 1} \frac{1 - \mu^2}{\mu}\right) \left(1 + 2\mu + \frac{1}{\mu^2}\right),$$

$$\mu(M) = \sqrt{\frac{(\gamma - 1)M^2 + 2}{2\gamma M^2 + 1 - \gamma}},$$

$$\eta(M) = \frac{1}{2\gamma} \left\{ \left[\frac{\gamma(\gamma - 1)}{2} \right]^{1/2} + 1 \right\} \left\{ 1 - \frac{M_0^2}{M^2} \right\} + \frac{1}{2} \ln A,$$

where A is the local shock area (the "ray-tube") normalized by its initial value. The integration develops from an initially planar front, with M_0 the initial value of M and, following [7], was numerically handled by means of a time-marching method in a two-dimensional Lagrangian frame. Figure 3 shows an example of calculation with $M_0 = 2.9$, $\gamma = 1.4$ and $N = 100$ discretization points on the initial front.

This M_0 value is too small to represent that of an actual detonation, and in our GSD implementation, all coefficients were obtained from the Rankine-Hugoniot relations and the non-reactive perfect-gas equation of state (constant γ , no heat of reaction). The goal of this preliminary calculation was indeed to check whether GSD was capable to capture qualitatively the main features of the experimental observations, and as a matter of fact, the agreement is remarkably good. Specifically, a Mach front breaks away from the outer wall and eventually rotates with a constant height, that is at a constant distance to the outer wall. The front line shows a fold that we have interpreted as a triple point, of which the approximate trajectory is indicated by the

dashed red line in Figure 3. This line represents the inflection point separating the straight Mach stem and the curved shock, the latter propagating with a smaller velocity. This approach cannot capture downstream flow, there is no reflected shock or shear layer attached the triple point. Figures 4-a 4-b are plots of the Mach-front height and normal velocity at the outer wall as a function of angular position, respectively, measured from the diffraction point at the chamber entry channel. They indicate essentially constant front height and normal velocity beyond position 150 deg. Decreasing p_0 (or M_0) results in Mach stems that decay into an inverse Mach reflection and, finally, into a regular two-shocks reflection. Increasing p_0 results in Mach stems that grow until reaching the center body. This is the trend obtained in the experiments when p_0 was increased above the upper limit of the observation range of the Mach detonation regime.

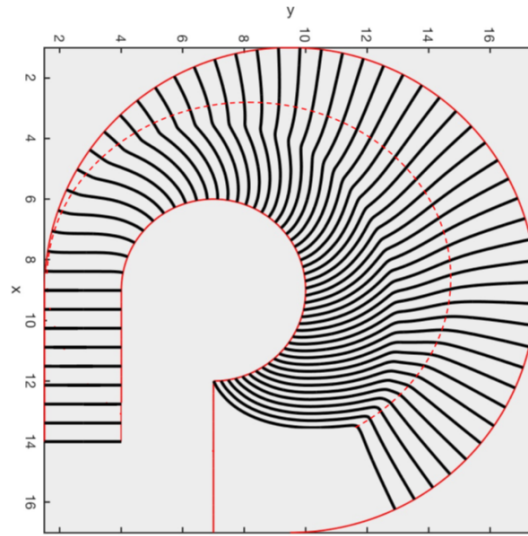


Figure 3: GSD modeling of shock transmission and propagation in a curved chamber ($M_0 = 2.9$).

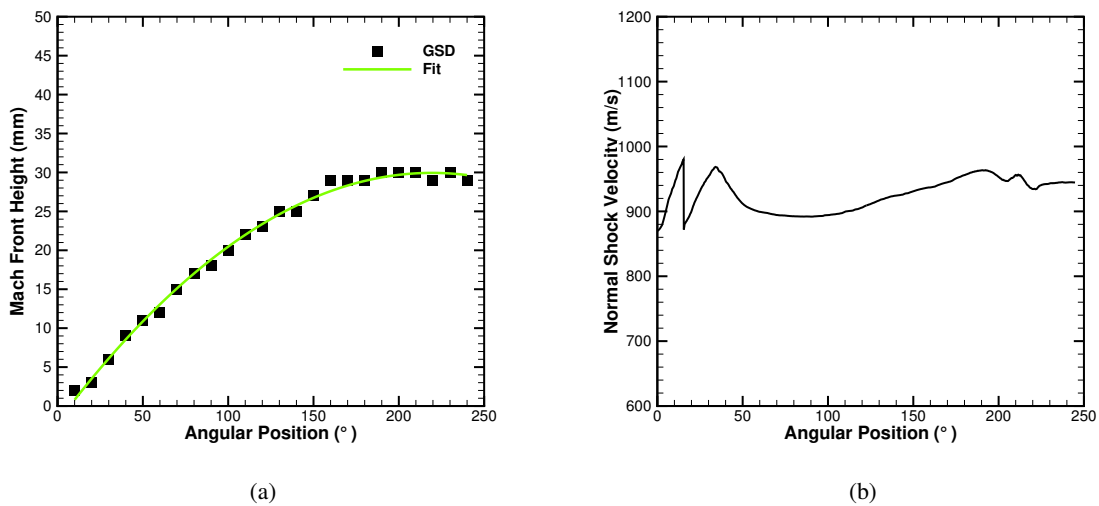


Figure 4: Mach stem height (a) and normal velocity of the shock at the outer wall (b) versus angular position.

4 Conclusion and perspectives

This preliminary GSD implementation was limited to non-reactive discontinuities but nevertheless substantiates our former interpretation [3, 4] that this specific regime is essentially self-similar, and thus mostly driven by geometry, and not by the chemical kinetics in the detonation reaction zone. Current modeling effort focuses on describing more realistically the Mach front as a fully-reactive discontinuity. This entails modifying the coefficients of the $A-M$ relation so as to include the effects of the heat of reaction by means of the reactive perfect-gas equation of state, the diffracted shock remaining a non-reactive discontinuity, and the shift from one equation of state to the other being determined by tracking the triple-point position. Based on this more realistic modeling a self-similar criterion will be checked. Little qualitative changes is expected compared to the inert case. Current experimental effort is directed towards collecting more data for several reactive mixtures and initial conditions in order to draw more general conclusions and generate non-dimensional information on the existence domain of this over driven detonation regime. Also in progress is a PLIF implementation to obtain more information on the reactivity distribution behind the diffracted shock and in the vicinity of the contact discontinuity behind the triple point.

Acknowledgement: this work is part of the CAPA research program on Alternative Combustion Modes for Air-breathing Propulsion supported by SAFRAN, MBDA and the French National Agency (ANR).

References

- [1] Hansmetzger S., Zitoun R., Vidal P., A study of continuous rotation modes of detonation in an annular chamber with constant or increasing section, *Shock Waves* 28, 1065-1078 (2018).
- [2] Anand V., St. George A., Gutmark, E., Hollow rotating detonation combustor, 54th AIAA Aerospace Sciences Meeting, San Diego, (2016)
- [3] Rodriguez V., Vidal P., Zitoun R., Experimental observations of semi-confined steadily-rotating detonation, *Proceedings of the 26th International Colloquium on the Dynamics of Explosions and Reactive Systems*, Boston, (2017)
- [4] Rodriguez V., Jourdain C., Vidal P., Zitoun R., An experimental evidence of steadily-rotating overdriven detonation, *Comb. and Flame*, Accepted (2019).
- [5] Hornung H., Regular and Mach reflection of shock waves, *Ann. Rev., Fluid Mech.*, 18, 33-58 (1986)
- [6] Whitham G.B., *Linear and nonlinear waves*, Wiley (Interscience) (1974).
- [7] Henshaw W.D., Smyth N.F., Schwendeman D.W., Numerical shock propagation using Geometrical Shock Dynamics, *Journal of Fluid Mechanics*, 171, 519-545 (1986).
- [8] Ridoux J., Lardjane N., Monasse L., Coulouvrat F., Comparison of Geometrical Shock Dynamics and kinematic models for shock wave propagation, *Shock Waves*, 28(2), 401-416 (2018).
- [9] Milton B.E., Mach reflection using ray-shock theory, *AIAA Journal*, 13(11), 1531-1533 (1975).
- [10] Ndebele B.B., Skews B.W., Paton R.T., On the propagation of curved shock waves using Geometrical Shock Dynamics, 30th International Symposium on Shock Waves 2, Tel-Aviv (2015).